'89 KACC 1989. 10. 27~28

SIGNAL PROCESSING TO MEASUREMENTS OF DYNAMIC TORQUE BY USE OF MAGNETIC LATTICE

Toshiyuki Asakura and Masaru Danno

Faculty of Engineering, Fukui University
Fukui, 910, Japan

Abstract This paper presents the preliminary studies on measurements of dynamic torque in the rotating shaft by utilizing the magnetic lattice. The intensity of torque can be detected as the phase differences between two magnetic sinusoidal signals recorded on magnetic tapes wound on the shaft. This research describes, from the data concerning with phase differences including noise, a method of signal processing to estimate the true value of the torque.

1. Introduction

In this paper, the preliminary studies are developed on measurements of dynamic torque in the rotating shaft by utilizing the magnetic lattice. The intensity of torque is proportional to the relative angular displacement of two positions on the shaft at some distance apart. This displacement can be detected as the phase differences between two magnetic sinusoidal signals which are recorded on magnetic tapes wound on those two positions. The purpose of this research developes, from data concerning with phase differences including noise, a method of signal processing to estimate the true value of the torque through the application of Kalman filter. There are few papers with respect to the application of Kalman filter to the torque measurement, except some examples concerning with instrumentation system.[1][2]

First, the principle of the measurement is explained with the experimental device, in which the characteristics of the device is clarified. Second, the guideline for the design of the torquemeter is illustrated, taking the case of drilling machine. Third, a method of signal processing is proposed to obtain the true value of the torque. For this purpose, the mathematical model of the torque dynamics can be represented by the state equation, from which the Kalman filter algorithms are derived. Finally, using both simulated and real data, it is ascertained that the true value of the torque can be estimated accurately by the Kalman filter.

2. Principle of Measurement and Experimental Device

2.1 Principle of Measurement

As shown in Fig.1, when the torque T is applied on the shaft with diameter d and length ℓ, the relative angular displacement between two positions A and B is given by

$$\theta = 32\ell T/\pi d^4 G. \qquad (2.1)$$

Now, magnetic tapes are wound on both circumstances A and B of the shaft, on which n pieces of magnetic lattice (sinusoidal signal with the wave length λ) are magnetized, respectively. Then, the number of the waves in a round of the shaft is,

$$n = \pi d/\lambda. \qquad (2.2)$$

From each magnetic heads corresponding to two magnetic tapes, the output signals E_a

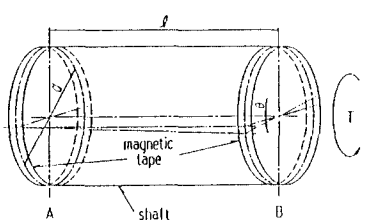

Fig.1 Explanation of torque detection

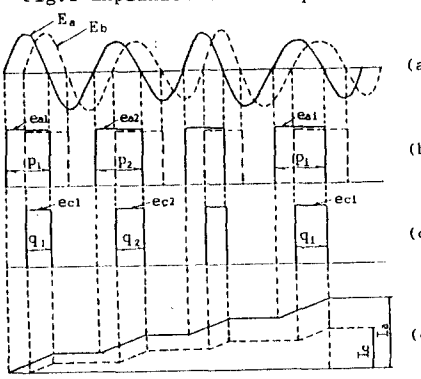

Fig.2 Signal processing of phase difference

and E_b can be obtained as,

$$E_a = z_1 \sin n\omega t \qquad (2.3)$$

and

$$E_b = z_2 \sin n(\omega t-\theta)$$
$$= z_2 \sin n(n\omega t-n\frac{32\ell}{\pi d^4 G}T). \qquad (2.4)$$

The relative phase difference ϕ between E_a and E_b and the torque T may be written by the following relation,

$$\phi = 32\ell nT/\pi d^4 G. \qquad (2.5)$$

From Eq.(2.5), the torque T can be obtained by measuring the phase difference ϕ. Also, the improvement of sensitivity may be possible by making λ small.

Next, the method to explore ϕ in (2.5) is illustrated using Fig.2. Both the voltages E_a and E_b in Fig.2(a), which were obtained from each magnetic heads, are translated into the square waves as shown in Fig.2(b), the logical sum of them operated as Fig.2(c) and the integral results I_a and I_b obtained from each e_{ai} and e_{ci} as Fig.2(d).

Using I_a and I_c, the phase difference ϕ becomes,

$$\phi = \pi(1 - I_c/I_a), \qquad (2.6)$$

where $I_c/I_a = \sum_{i=1}^{k} (q_i/p_i)$.

2.2 Experimental Device Based on the above principle, the torquemeter was made on trial and equipped with the rotating shaft of a bench lathe as shown in Fig.3. The bench lathe used here is to have the rotating frequency 10∿40 rps and the output 140w. For the increase of measuring accuracy, two rings with diameter D are equipped at both ends of the rotating shaft. The magnetic tapes were wound on these rings, on which sinusoidal signals were recorded with the wave length 157μm. Corresponding to each magnetic tapes, magnetic heads were set, from which the signal detection was carried out.

The signal processing circuit to explore the phase difference from detected signals is shown in Fig.4. That is, the output signals E_a and E_b, obtained from regenerated heads, are amplified, their noises are excluded through filters and transformed into rectangular signals by the converter. From both signals (e_{ai} and e_{bi}) including the phase difference, the logic sum e_{ci} is obtained through the gate circuit. As it is necessary to calculate the ratio of p_i and q_i to obtain the phase difference, we have outputs cp_i and cq_i by interporating e_{ai} and e_{ci} into the integrater. By these signals passing through both the division circuit and sample & hold one, the value I_c/I_a may be explored and then the phase difference ϕ obtained from Eq.(2.6). Here, the integral time of e_{ai} and e_{ci}, that is, the measuring interval of the torque was set to be about 4ms.

Through experiments of the characteristics with respect to the device on trial, it was ascertained that the signal processing circuit has sufficient linearities between the phase difference ϕ and the output voltage and between the displacement of the head and the output one. These results are shown in Figs.5 and 6.

3. Guideline for Design

As the object of torque measurement, we shall, for instance, consider a drilling machine. When we use a drill with the diameter 10 ∿ 50 mm, torque values which are necessaty to the drilling for various materials may be considered to be about 4 ∿ 480 N·m. On the otherhand, there is a drilling machine with low capacity for high-speed rotation, which is, for instance, 0.2∿0.5N·m and maximum rotational frequency 250 rps. For this purpose, the strain-gauge type torque

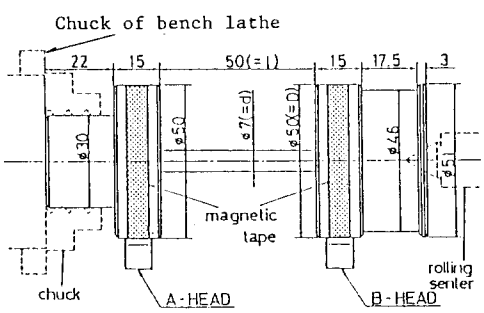

Fig.3 Signal detection part

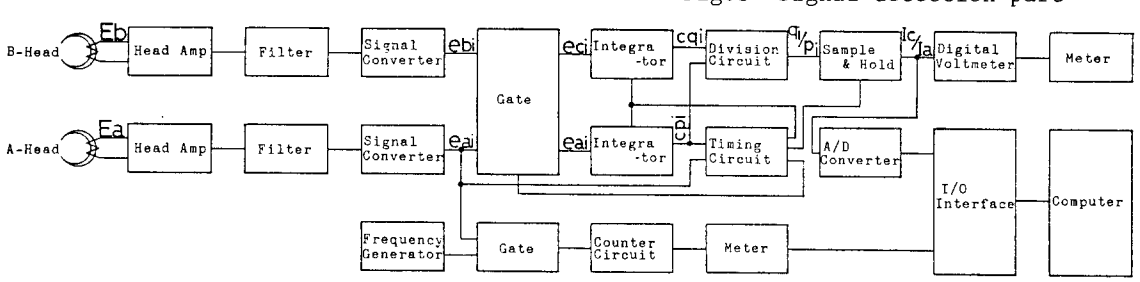

Fig.4 Signal processing circuit of phase difference

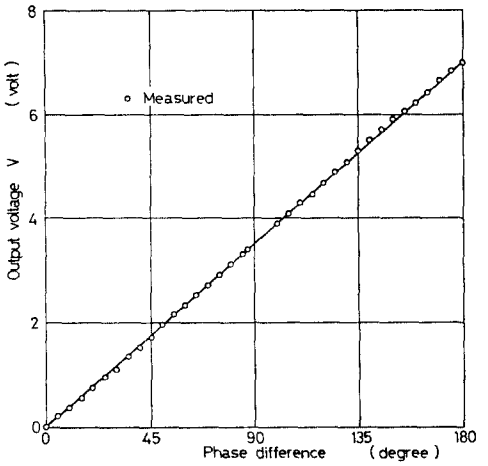

Fig.5 Relation between phase difference and output voltage

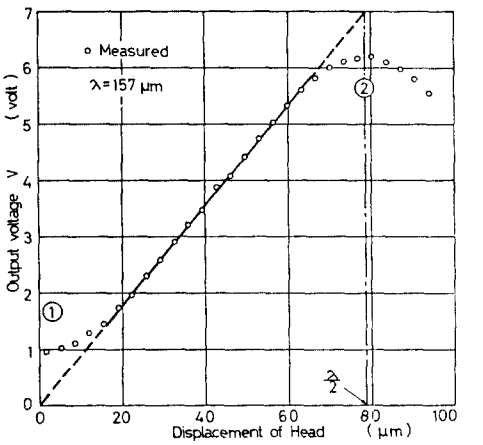

Fig.6 Relation between displacement of head and output voltage

transformer is used. [3] Thus, the torquemeter must have demands in the wide range from high capacity and low one.

In this experiment, enlarging the diameter of parts with magnetized tape at both ends of the shaft, the sensitivity increases. For such cases, the performance of measurements will be examined.

Both the detectable torque capacity and the measurable rotational frequency of the shaft depend on a diameter d, the distance between two tapes ℓ, the wave length of the magnetic lattice λ, of the rotating shaft to be measured. For instance, making the wave length λ small, it becomes possible to detect the minute torque. However, as the measuring frequency becomes high, it is difficult to measure the torque in the high speed rotation. Also, letting the distance between two tapes long, the sensitivity becomes high but the diameter of the shaft large, it is impossible to detect the minute torque. On the otherhand, these results are desirable from the viewpoint of the response frequency, since the natural frequency of the twisted vibration becomes large. Thus, various parameters bring complex effects to the performance of measurements. Then, we prepared the diagram which gives a standard for the design of a torquemeter, as shown in Fig. 7. That is, given the wave length λ of the magnetic lattice, Eq.(2.5) can be written, using $n=\pi D/\lambda$ instead of Eq.(2.2), by

$$T = \frac{\pi D}{32}\frac{\lambda}{D}\left(\frac{d^4}{\ell}\right) , \qquad (3\text{-}1)$$

where $G=8.1\times10^{10}\ N/m^2$ in the case of mild or hard steel. In Fig.7, the break line parallel to a holizontal axis show the limit of the shaft in the case d is given, considering the strength of the shaft. This limit is given by

$$T_{max} = \tau_a \times \pi d^3/16. \qquad (3\text{-}2)$$

Here, τ_a represents the allowable shearing stress and estimated as $\tau_a=2.0\times10^7 N/m^2$ [4] in the case of hard steel. For example, we shall consider the case where d=0.01m and ℓ=0.05m. Then, from Fig.7, it can be seen that the limit of the measurable torque is about $T_{max}=3.80N\cdot m$ and the ratio between the wave length λ of the magnetic lattice and the shaft diameter wound by the magnetic tape is suitable if it is selected to be about $(\lambda/D)=3\times10^{-3}$.

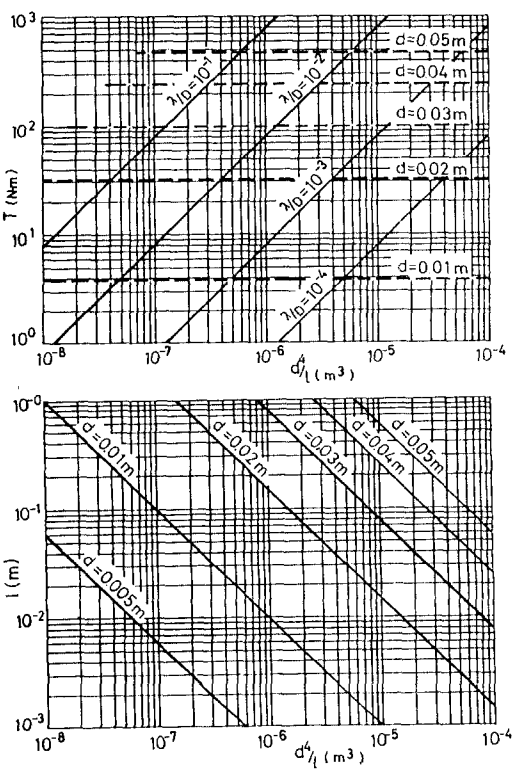

Fig.7 Design principle for torquemeter

4. Signal Processing to Measurements

Since observed signals concerning with phase differences include, more or less, both noisy elements and transient responses based on the force of inertia, it is generally difficult to know directly the value of dynamic torque from the output signals. Then, as a method of signal processing, an approach is developed to measure the true value of torque through the application of Kalman filter.[5]

For this purpose, we shall consider the dynamical equation with respect to the torque variation, based on the physical model of the measuring device in Fig. 3. In the case where the load is applied to the shaft, we suppose that the mathematical model of the dynamics with respect to the phase differences may be described by the following differential equation,

$$\frac{d^2\phi(t)}{dt^2}+\alpha\frac{d\phi(t)}{dt}+\beta\phi(t)=U(t)+v(t), \quad (4\text{-}1)$$

where α and β are inherent constants of the device and $v(t)$ is a noise element included in magnetized sinusoidal signals. Also, $U(t)$ is the equivalent value of the torque, which is given by

$$U(t)=T\cdot(\pi D/\lambda)(1/I_m), \quad (4\text{-}2)$$

where I_m is a moment of inertia of the rotating shaft. The observation mechanism, from which the phase difference is taken out as the voltage, may be represented by

$$y(t)=\phi(t)+w(t), \quad (4\text{-}3)$$

where $w(t)$ is an observation noise. Letting $x_1=\phi$, $x_2=\dot{x}_1$ and $x_3=U$, Equations (4-1) and (4-3) are written by the following state equation,

$$\dot{x}=Ax+Bv \quad (4\text{-}4)$$

$$y=Cx+w \quad (4\text{-}5)$$

where

$$A=\begin{bmatrix}0&1&0\\-\beta&-\alpha&1\\0&0&0\end{bmatrix},\quad B=\begin{bmatrix}0\\1\\0\end{bmatrix}, \quad (4\text{-}6)$$

$$C=[\,1\ 0\ 0\,].$$

Representing Eqs.(4-4) and (4-5) by the discrete-time system,[6] it follows that

$$x(k+1)=\Phi(k)x(k)+L(k)v(k) \quad (4\text{-}7)$$

$$y(k)=C(k)x(k)+w(k) \quad (4\text{-}8)$$

where $\Phi(k)$ and $L(k)$ are given in Appendix A. Also, both $v(k)$ and $w(k)$ are assummed to be white Gaussian random processes with following properties;

$$E[v(k)]=E[w(k)]=0$$

$$E[v(k)v(j)^T]=Q(k)\delta_{kj} \quad (4\text{-}9)$$

$$E[w(k)w(j)^T]=R(k)\delta_{kj},$$

where δ_{kj} is a Kronecher's delta function, and $Q(k)$ and $R(k)$ are constants.

Then, using Eqs.(4-7) and (4-8), the discrete-time Kalman filter[7] can be deribed as

$$\hat{x}(k+1)=\Phi(k)\hat{x}(k|k-1)-K(k)[y(k)-C(k)\hat{x}(k|k-1)] \quad (4\text{-}10)$$

$$K_1(k)=-P(k|k-1)C(k)^TV(k)^{-1} \quad (4\text{-}11)$$

$$V(k)=C(k)P(k|k-1)C(k)^T+R(k) \quad (4\text{-}12)$$

$$K(k)=\Phi(k)K_1(k) \quad (4\text{-}13)$$

$$P(k)=[I-K_1(k)C(k)]P(k|k-1) \quad (4\text{-}14)$$

$$P(k+1|k)=\Phi(k)P(k)\Phi(k)^T+L(k)Q(k)L(k)^T. \quad (4\text{-}15)$$

Also, initial conditions are given by

$$\hat{x}(k_0|k_0-1)=E[x(k_0)]$$

$$P(k_0|k_0-1)=E[\{x(k_0)-x(k_0-1)\}\times\{x(k_0)-x(k_0-1)\}^T], \quad (4\text{-}16)$$

where $P(k)$ is an error covariance matrix such as,

$$P(k|k-1)=E[\{x(k)-x(k-1)\}\times\{x(k)-x(k-1)\}^T]. \quad (4\text{-}17)$$

From above algorithms, the calculation of estimation may be carried out by Eq.(4-10), after calculating Kalman gain K.

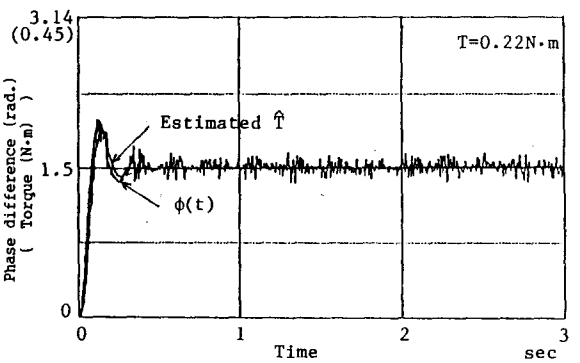

Fig.8 Simulated data and its estimated result

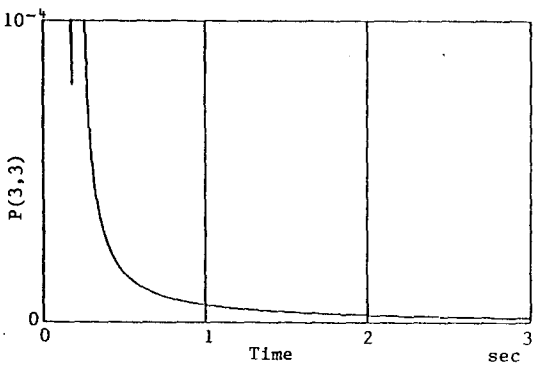

Fig.9 Error covariance

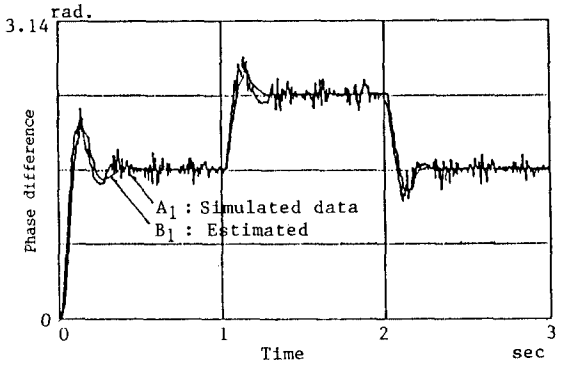

Fig.10 Estimated result for a step-like torque variation

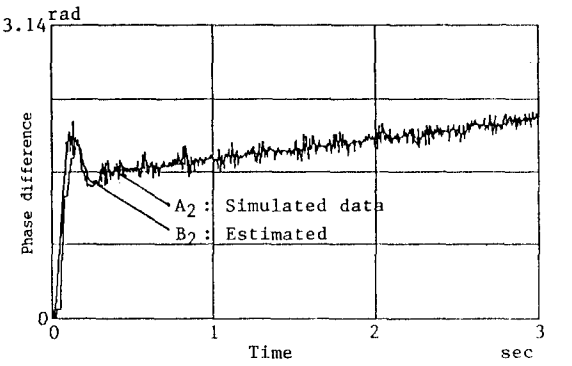

Fig.11 Estimated result for a ramp-like torque variation

5. Simulation Experiments

Using data concerning with phase differences including noise, simulation experiments are performed to estimate the true value of the torque by applying the Kalman filter. The simulation data $\phi(t)$, supposed that both the step-like and ramp-like torques are applied on the rotating shaft, are generated from Eqs.(4-7) and (4-8). Also, the calculation of Kalman filter from Eq.(4-10) to (4-15) is carried out by using C-langauge [8] to realize the real-time signal processing. A set of parameters in Eqs.(4-7) and (4-8) has been determined, from the experimental device, as

$$D=50\text{mm},\ \ell=50\text{mm},\ I_m=182\text{kg}\cdot\text{mm}^2,$$
$$\lambda=157\mu\text{m},\ \alpha=5,10\text{s}^{-1},\ \beta=787\text{s}^{-1}, \qquad (5\text{-}1)$$
$$R=4\times10^{-2}\text{s}^{-1},\ Q=1.8\times10^{-2}\text{s}^{-1}.$$

Applying these parameters to Kalman filter algorithm, simulation experiments have been performed. Figure 8 shows the simulated data $\phi(t)(=x_1(t))$ and its estimated result $T(=\hat{x}_3(t))$ in the case where $T=0.22\text{N}\cdot\text{m}$ is applied. Although the $x_1(t)$-process becomes a random vibration, the $\hat{x}_3(t)$-process shows very good convergence for the estimate of $T=0.22\text{N}\cdot\text{m}$. The error covariance $P(3,3)$ with respect to $\hat{x}_3(t)$-process is, in this case, shown in Fig.9, which shows the justification of the estimated result. Figure 10 shows the estimated result in the case where the magnitude of the torque changes on the way, that is, from $T=0.22\text{N}\cdot\text{m}$ to $T=0.33\text{N}\cdot\text{m}$ at $t=1$(sec) and also, returns to $T=0.22\text{N}\cdot\text{m}$ at $t=2$(sec). Furthermore, Fig.11 shows, similarly, the estimated one in the case where a ramp-like torque variation is acted on the shaft. In Figs.10 and 11, A_1 and A_2 are the simulated data and B_1 and and B_2 the estimated results. From these results, it was ascertained that the true value of the torque can be estimated within 0.5sec at sufficient accuracy.

Next, the signal processing time for the estimation of the dynamic torque become, letting the sampling frequency be 0.01sec, 2.78sec in cases of Figs.10 and 11. Here, the PC-9801VX was used. Accordingly, it was certified that the real time data processing could be possible, connecting the experimental device with the digital computer on line.

Furthermore, this method has been applied to real data obtained by inflicting the load on the rotating shaft of a bench lathe. At result, though the detection mechanism must be somewhat improved, the good estimated results have been obtained similar to the simulated ones.

6. Conclusions

For Measurements of dynamic torque in the rotating shaft, a new method using magnetic lattice has been proposed and a guideline for the design of torquemeter has been given. This method can be possible to measure the torque in a wide range with high accuracy by choosing arbitrarily the wave length λ of the sinusoidal signals, comparing with the usual torsion bar torquemeter. Applying the torquemeter made in trial to a bench lathe, both the theoretical and experimental considerations were performed.

(1) As the detected signals include both system and observed noises, the true values of the dynamic torque were estimated based on the signal processing using the Kalman filter.

(2) For this purpose, a mathematical model of the torque dynamics was presented by the state equation, from which the Kalman filter algorithm was derived. Using the simulated data generated by the state equation, it was ascertained that the true value of the torque could be estimated accurately.

(3) This method was applied to real data obtained from the rotating shaft of a bench lathe and good estimated results were obtained, with the possibility of the practical use.

Acknowledgments

The authors wish to thank Mr T.Kurose and Mr S.Morinaga for their assistance. This research was partly supported by the scientific research fund from the Ministry of Education and Shimadzu science foundation, for which the authors wish to express their sincere gratitude.

Appendix A

Derivation of $\Phi(k)$ and $L(k)$:

The $\Phi(k)$ and $L(k)$ can be caluculated by using Sylvester's theorem [6] as,

$$\Phi(k) = \begin{bmatrix} \phi_{11} & \phi_{12} & \phi_{13} \\ \phi_{21} & \phi_{22} & \phi_{23} \\ \phi_{31} & \phi_{32} & \phi_{33} \end{bmatrix} \qquad \text{(A-1)}$$

$$L(k) = [\, L_1 \; L_2 \; L_3 \,]. \qquad \text{(A-2)}$$

Letting s be a sampling interval, each elements of (A-1) and (A-2) are;

$$\phi_{11}=\exp(-\alpha s/2)\cos(\sqrt{4\beta-\alpha^2}\,s/2)+(2\beta \times\sqrt{4\beta-\alpha^2})\exp(-\alpha s/2)\sin(\sqrt{4\beta-\alpha^2}\,s/2)$$

$$\phi_{12}=2\exp(-\alpha s/2)/\sqrt{4\beta-\alpha^2}\sin(\sqrt{4\beta-\alpha^2}\,s/2)$$

$$\phi_{13}=(1/\beta)-\exp(-\alpha s/2)[(1/\beta)\cos(\sqrt{4\beta-\alpha^2}\,s/2)+(\alpha/\beta\sqrt{4\beta-\alpha^2})\sin(\sqrt{4\beta-\alpha^2}\,s/2)]$$

$$\phi_{21}=-\exp(-\alpha s/2)(\sqrt{4\beta-\alpha^2})+(\alpha/\beta\sqrt{4\beta-\alpha^2}) \times\sin(\sqrt{4\beta-\alpha^2}\,s/2)$$

$$\phi_{22}=\exp(-\alpha s/2)[\cos(\sqrt{4\beta-\alpha^2}\,s/2) -2\{(-\beta+\alpha^2/2)(\alpha/2\beta\sqrt{4\beta-\alpha^2}) +\alpha\sqrt{4\beta-\alpha^2})/4\beta\}\cdot\sin(\sqrt{4\beta-\alpha^2}\,s/2)]$$

$$\phi_{23}=(\alpha^2/\beta\sqrt{4\beta-\alpha^2})\exp(-\alpha s/2) \times\sin(\sqrt{4\beta-\alpha^2}\,s/2)$$

$$\phi_{31}=\phi_{32}=0, \qquad \phi_{33}=1$$

$$L_1=(\alpha/\beta\sqrt{4\beta-\alpha^2})[(\sqrt{4\beta-\alpha^2})/\alpha)(1 -\exp(-\alpha s/2)\cos(\sqrt{4\beta-\alpha^2}\,s/2) -\exp(-\alpha s/2)\sin(\sqrt{4\beta-\alpha^2}\,s/2)$$

$$L_2=\exp(-\alpha s/2)[1/4\beta^2\sqrt{4\beta-\alpha^2})\{2+ \times[2\beta-(1/\beta)]\sin(\sqrt{4\beta-\alpha^2}\,s/2\} +\alpha(\alpha+1)/2\beta^2]$$

$$L_3=0.$$

References

(1) J.M.Freeman,F.N.Hassan & D.Morton, Kalman filter estimation of electrical machine parameters,Int.J.Control, 43-1(1986),pp.305-312

(2) Y.Fujinaka,Strain measurement by magnetic tape, Pro.11th WCNDT,Vol.1(1985),pp.629-635

(3) T.Naitō,Industrial instrumentation handbook,Asakura shoten,(1976),pp. 143-147

(4) K.Ohnishi,Machine design and drafting handbook,Rikōgaku Co Ltd.,4-4(1980) pp.3-5(4)

(5) B.D.O.Anderson and J.B.Moore,Optimal filtering,Prentice Hall(1979)

(6) M.Gopal,Modern control system theory, Wily Eastern Ltd.,(1984),pp.30-31

(7) A.H.Jazwinski,Stochastic processes and filtering theory,Academic Press (New York),(1970),pp.195-200

(8) B.W.Kernigham and D.M.Ritche, The C programing language,Prentice Hall, (1970)